Pharm Res (2014) 31:2287–2296
DOI 10.1007/s11095-014-1324-4

RESEARCH PAPER

A Mechanism Enhancing Macromolecule Transport Through Paracellular Spaces Induced by Poly-L-Arginine: Poly-L-Arginine Induces the Internalization of Tight Junction Proteins via Clathrin-Mediated Endocytosis

Tsutomu Yamaki • Yusuke Kamiya • Kazuo Ohtake • Masaki Uchida • Toshinobu Seki • Hideo Ueda • Jun Kobayashi • Yasunori Morimoto • Hideshi Natsume

Received: 15 October 2013 / Accepted: 28 January 2014 / Published online: 5 March 2014

ABSTRACT

Purpose Poly-L-arginine (PLA) enhances the paracellular permeability of the Caco-2 cell monolayer to hydrophilic macromolecules by disappearance of tight junction (TJ) proteins from cell–cell junctions. However, the mechanism of the disappearance of TJ proteins in response to PLA has been unclear. In this study, we investigated the mechanism of disappearance of TJ proteins from cell–cell junctions after the application of PLA to Caco-2 cell monolayers.

Methods The membrane conductance (G_t), FITC-dextran (FD-4) permeability, and localization of TJ proteins were examined after the treatment of Caco-2 cell monolayers with PLA in the presence of various endocytosis inhibitors. In addition, the localization of endosome marker proteins was also observed.

Results Clathrin-mediated endocytosis inhibitors suppressed the increase in G_t and P_{app} of FD-4 induced by PLA, and also significantly suppressed the disappearance of TJ proteins induced by PLA. Furthermore, occludin, one of the TJ proteins, colocalized with early endosome and recycling endosomes after the internalization of occludin induced by PLA, and then was recycled to the cell–cell junctions.

Conclusion PLA induced the transient internalization of TJ proteins in cell–cell junctions via clathrin-mediated endocytosis, subsequently increasing the permeability of the Caco-2 cell monolayer to FD-4 via a paracellular route.

T. Yamaki • Y. Kamiya • K. Ohtake • M. Uchida • T. Seki • H. Ueda • J. Kobayashi • Y. Morimoto • H. Natsume (✉)
Faculty of Pharmaceutical Sciences, Josai University, 1-1 Keyakidai Sakado, Saitama 350-0295, Japan
e-mail: natsume@josai.ac.jp

T. Seki • Y. Morimoto • H. Natsume
Research Institute of TTS Technology, Josai University, 1-1 Keyakidai Sakado, Saitama 350-0295, Japan

KEY WORDS absorption enhancer · drug delivery · hydrophilic-macromolecules · poly-L-arginine · tight junction

INTRODUCTION

It has recently been shown that polycationic materials, such as poly-L-arginine, poly-L-lysine, protamine, chitosan and N-trimethyl chitosan, have the potential to promote the transmucosal delivery of macromolecules without inducing severe epithelial toxicity (1–4). Of these, PLA and chitosan predominantly increase the paracellular permeability to hydrophilic macromolecules across excised rabbit nasal mucosa and Caco-2 cell monolayers (5,6). Ohtake *et al.* reported that the enhanced paracellular permeability induced by PLA involves the dispersion of tight junction (TJ) and adherens junction (AJ) proteins into the cytoplasm through the cell–cell junctions. In addition, PLA enhances the paracellular permeability via the serine/threonine phosphorylation of ZO-1 and tyrosine dephosphorylation of occludin in the excised rabbit nasal mucosa *in vitro* (7). However, it was difficult to further analyze the mechanism underlying the TJ disassembly induced by PLA in this model because of the lack of antibody crossover between rabbits and other animals and the low amount of TJ proteins that could be detected by an immunoblot analysis.

TJs are found between adjacent cells, and the occludin and claudin families of proteins, which include four transmembrane domain proteins, are distributed throughout the TJs (8–10). Occludin and claudin play an important role in the rate-limiting step of the permeation of ions and other solutes through the paracellular space (11,12). It was recently reported that a four transmembrane domain protein called tricellulin was located at the intersection where three adjacent cells meet (tricellular tight junctions) (13). These TJ structural

proteins cooperatively form TJ strands. PLA may be able to enhance the permeability of cell layers to macromolecules by altering the distribution of claudin and tricellulin, as well as occludin and ZO-1.

In our current study, we performed further experiments to examine the effects of PLA using human Caco-2 cell monolayers. PLA induced an increase in FITC-dextran (MW: 4 kDa, FD-4) permeation through Caco-2 cell monolayers in a concentration-dependent manner (14). This was found to be mainly due to the paracellular permeability of Caco-2 monolayers to FD-4, and involved the dispersion of TJ proteins, including ZO-1, claudin-4, occludin and tricellulin, from cell–cell junctions to the subcellular space. Of these four proteins, occludin appeared to mainly play a role in the enhanced permeation of hydrophilic macromolecules through Caco-2 cell monolayers following PLA exposure, because the kinetic analyses of TJ proteins showed these proteins to be dispersed when the FD-4 permeability increased. Furthermore, the disappearance of TJ proteins from cell–cell junctions induced by PLA had almost no association with the degradation of TJ proteins, as demonstrated by a Western blot analysis with whole cell lysates, thus suggesting that they are lost due to their internalization in the subcellular space.

It has previously been shown that several types of endocytosis can lead to the internalization of TJ proteins from cell–cell junctions to the subcellular spaces (15–18). These include clathrin- and caveolae-mediated endocytosis and macropinocytosis (19). Following Ca^{2+} depletion and vascular endothelial growth factor (VEGF) treatment, the distribution of TJ proteins was associated with clathrin-mediated endocytosis (15,16). It is known that, following the exposure of brain endothelial cells to a chemokine ligand (CC ligand 2), occludin and claudin-4 are internalized by caveolae-mediated endocytosis (17). Furthermore, ZO-1 and claudin-1 undergo macropinocytosis in response to stimuli such as TNF-alpha and -beta in T84 intestinal epithelial cells (18). PLA was also found to be associated with these endocytosis processes which induce the internalization of TJ proteins.

It has been demonstrated that TJ proteins are delivered to the early endosome after cellular uptake (20). They are then sorted selectively and distributed between late endosomes and recycling endosomes. The late endosomes carry out the degradation of these proteins, whereas the recycling endosomes deliver the proteins to the plasma membrane to reconstitute the TJ complex (15). We hypothesized that, following PLA exposure, the TJ proteins distributed from cell–cell junctions to the subcellular spaces may be delivered to these endosomes.

In the present study, we first investigated which type(s) of endocytosis was involved in the internalization of TJ proteins after the exposure of Caco-2 cells to PLA using different inhibitors of endocytosis, and performed an immunofluoresent observation of TJ proteins while monitoring the membrane conductance (G_t) and paracellular permeability of the Caco-2 cell monolayer to a model hydrophilic macromolecule, FD-4. Second, we determined the location of occludin in the storage compartment of Caco-2 cells after PLA exposure, because occludin was the protein that was found to play the most important role in the enhanced permeability to FD-4 induced by PLA. We provided the first evidence of the disappearance and recycling of TJ proteins in cell–cell junctions after treatment of Caco-2 cells with PLA, leading to the increased paracellular permeability of macromolecules.

MATERIALS AND METHODS

Materials

Poly-L-arginine (MW: 44,300), fluorescein-isothiocyanate dextran (FD-4, MW: 3,850), monodansylcadaverine (MDC), filipin, methyl-β-cyclodextrin (MβCD) and wortmannin (Wort) were obtained from Sigma Aldrich (St. Louis, MO). Chlorpromazine (CP) was purchased from Merck (Billerica, MA). Erythritol was purchased from Wako Chemicals (Osaka, Japan). Caco-2 cells were purchased from the American Type Culture Collection (Manassas, VA). The cell culture reagents and supplies were purchased from Invitrogen (Carlsbad, CA). All other reagents were of analytical grade.

Antibodies

Mouse monoclonal anti-occludin, anti-claudin-4, rabbit polyclonal anti-ZO-1, anti-tricellulin, anti-EEA1, Alexa fluor-488 anti-rabbit-IgG, Alexa fluor-488 anti-chicken IgG, and Alexa fluor-594 anti-mouse IgG were purchased from Invitrogen. Anti-LAMP-1 was purchased from Millipore (Billerica, MA). Anti-rab11 and anti-clathrin heavy chain were purchased from Cell Signaling Technology (Danvers, MA). The antibodies were used at the following dilutions during the immunofluorescence microscopy study: rab11 and clathrin heavy chain, 1:100; ZO-1 and tricellulin, 1:125; occludin, claudin-4, and LAMP-1, 1:250; EEA1, 400:1; and secondary antibody, 1:500.

Cell Culture

Caco-2 cells were maintained in Dulbecco's modified Eagle's medium (DMEM) supplemented with 10% fetal bovine serum, 1% non-essential amino acids (NEAA), 2% Gluta-MAX, 2% antibiotic-antimycotic at 37°C and were used for experimental purposes between passages 60 and 70. The cells were subcultured by partial digestion with 0.25% trypsin-EDTA. A total of 1×10^5 cells per cm^2 were seeded on polycarbonate Transwell membranes (24 mm; Corning, Lowell, MA), and used for experiments 21–28 days after seeding.

Treatment of Caco-2 Cell Monolayers with Endocytosis Inhibitors

Caco-2 cell monolayers were washed twice with Hank's balanced salt solution (HBSS), and the DMEM culture medium was replaced with HBSS or HBSS containing each of the inhibitors of endocytosis according to the previously reported studies (clathrin-mediated inhibitors: CP 30 μM and MDC 300 μM, caveolae-mediated inhibitors: filipin 5 μM and MβCD 5 mM, macropinocytosis inhibitor: Wort 100 nM) (16,18,21,22). Caco-2 cell monolayers were treated with these inhibitors for 60 min while monitoring the G_t at 37°C.

Determination of the G_t

The transepithelial electrical resistance (TEER) was measured using a Millicell-ERS device (Millipore, Billerica, MA) according to the manufacturer's protocol, and was calculated in units of ohms·cm^2 by multiplying it by the surface area of the monolayer. The cell monolayers were used for experiments when they provided a TEER of >500Ω·cm^2. The resistance of the polycarbonate membrane in the Transwell was subtracted from all readings. Caco-2 cell monolayers were washed twice with HBSS, and the DMEM was replaced with HBSS or HBSS containing the endocytosis inhibitors. Thereafter, PLA (100 μg/mL) was added to the apical side of the Caco-2 cell monolayer in the presence or absence of these inhibitors. The TEER was measured at 0, 15, 30, 45, 60, 90 and 120 min after the application of PLA at 37°C, and the average TEER was calculated from the values at 60 to 120 min. Each TEER was also converted to the membrane conductance (G_t = 1/TEER, mS/cm^2) and the ratio of the G_t in the treatment group to that in the control group (G_t ratio) was calculated.

FD-4 and Erythritol Permeation Studies

An FD-4 permeation study was performed as reported previously (14). Following the treatment of Caco-2 cell monolayers with HBSS or HBSS containing each endocytosis inhibitor, the apical bathing solution of the cell monolayers was changed to include PLA (100 μg/mL) and FD-4 (2.5 mg/mL), while cells were cultured at 37°C.

An erythritol permeation study was also done in the same manner. Following the treatment of Caco-2 cell monolayers with HBSS or HBSS containing CP, the apical bathing solution of the cell monolayers was changed to include PLA (100 μg/mL) and erythritol (45 mM), while cells were cultured at 37°C.

In these experiments, samples were collected from the basal side at 15, 30, 45, 60, 90 and 120 min, respectively, and the cumulative amounts of FD-4 and erythritol permeation per surface area (μg/cm^2) were calculated. The apparent permeability coefficients, P_{app} (cm/s), of FD-4 and erythritol were calculated as follows: $P_{app} = dQ/dt/(A \times C_0)$, where dQ/dt is the steady state permeation rate (μg/s) of FD-4 and erythritol, A is the surface area of the transwell (cm^2), and C_0 is the initial concentration (μg/cm^3) on the apical side. The ratio of the P_{app} in the treatment group to that in the control group (P_{app} ratio) was calculated.

One hundred microliters of FD-4-containing sample was diluted 100-fold with potassium dihydrogenphosphate-sodium borate buffer (pH 8.5). The fluorescence of FD-4 was then determined in an RF-1500 fluorescence spectrofluorometer (Shimadzu, Tokyo, Japan) with an excitation wavelength of 495 nm and an emission wavelength of 515 nm.

The amount of erythritol was determined with a dual-pump HPLC system (LC10, Shimadzu, Kyoto, Japan) with a Charged Aerosol Detector (CAD, ESA Biosciences, MA, USA)(23). A Shodex SC1011 column (SHOWADENKO, Tokyo, Japan) was used for the separation at 80°C. A pump provided water at 0.5 mL/min as the mobile phase, which passed through the injector and column. Another pump was used to provide acetonitrile at 0.5 mL/min. The water from the column and the acetonitrile were introduced into the CAD. Twenty microliters of each erythritol sample were injected for the analysis.

Immunofluorescence Microscopic Observation

The immunofluorescence microscopic observation of TJ proteins was performed as reported previously (24,25). In brief, after treatment under the various conditions described above, Caco-2 cell monolayers were washed twice with HBSS and fixed in acetone/methanol (1:1) at 4°C for 10 min at predetermined time points. The cell monolayers were blocked in TBS-T (10 mM Tris–HCl, pH 7.4, 150 mM NaCl, 0.1% Tween-20) with 3% skim milk for 1 h at room temperature, and were incubated with primary antibodies at 4°C overnight. The cell monolayers were then washed twice with TBS-T for 15 min, followed by incubation for 1 h with secondary antibodies. Fluorescence images were visualized using a confocal laser scanning microscope (CLSM) FV1000 (Olympus, Tokyo, Japan). The junctional fluorescence intensity of TJ proteins was determined according to the method described previously (8, 28). In brief, fluorescence images of samples were selected randomly, and the background of the images was calibrated using the threshold function of the Image J software program. The image was inverted, and the gray value was determined. The total junctional fluorescence intensity (mean gray value–background gray value) was calculated for each sample and was expressed as a percentage of the control.

Statistical Analysis

Each result is presented as the mean ± standard error (S.E.). The statistical analysis was performed using a one-way

ANOVA, together with Dunnett's test, to compare the data from different groups. A p value of <0.05 was considered to be significant.

RESULTS

Effects of Inhibitors of Endocytosis of the TJ Proteins Following PLA Treatment

To verify whether the increases in the G_t and FD-4 permeation via the paracellular pathway induced by PLA were associated with the endocytosis of TJ proteins, the G_t, the permeation of FD-4 and the distribution of TJ proteins were examined after the exposure of Caco-2 monolayers to PLA and different inhibitors of endocytosis. Figure 1 and Table I show the effects of the different inhibitors on the increase in the G_t ratio and P_{app} ratio of FD-4 induced by PLA in Caco-2 cell monolayers. After treatment with inhibitor alone, the G_t ratio and the P_{app} ratio of FD-4 were almost identical to those of the control, and the cell viability was also not changed (Fig. 1). The inhibitors of caveolae-mediated endocytosis (filipin and MβCD) and macropinocytosis (Wort) did not affect the increase in the G_t and P_{app} induced by PLA. In contrast, the PLA-induced P_{app} increase was significantly suppressed by the inhibitors of clathrin-mediated endocytosis (CP and MDC). The increase in the G_t was also inhibited significantly by these treatments, but to a lesser degree. In addition, cell viability was not affected by PLA in the presence of clathrin-mediated endocytosis inhibitors (data not shown).

Table I Effect of PLA on G_t and FD-4 P_{app} in Caco-2 Cell Monolayers

	G_t (mS/cm^2)	P_{app} (cm/s)
Control	0.65 ± 0.02	0.32 ± 0.04
PLA	3.19 ± 0.12	13.00 ± 0.92
Filipin + PLA	3.08 ± 0.07	12.07 ± 0.66
MβCD + PLA	2.93 ± 0.12	13.21 ± 1.60
Wort + PLA	2.98 ± 0.07	13.63 ± 0.79
CP + PLA	2.22 ± 0.09*	5.75 ± 0.30*
MDC + PLA	2.48 ± 0.06*	7.92 ± 0.68*

Each data point represents the mean ± S.E. ($n = 4$) *$p < 0.05$ *vs.* PLA

Figures 2 and 3 show the immunostaining images and intensities of TJ proteins 2 h after treatment with PLA following incubation of the cells with different inhibitors of endocytosis, respectively. Following the co-treatment with PLA and filipin, MβCD or Wort, all four TJ proteins examined (occludin, ZO-1, claudin-4 and tricellulin) disappeared from the cell–cell junctions. The intensities of these TJ proteins in cell–cell junctions were also reduced and were almost identical to the levels following the treatment with PLA alone (Fig. 3). On the other hand, these TJ proteins were still localized in the cell–cell junctions after PLA exposure following the treatment with CP and MDC (Fig. 2). In addition, the intensities of these TJ proteins in cell–cell junctions were almost the same as the control level following the co-treatment with PLA and CP or MDC (Fig. 3).

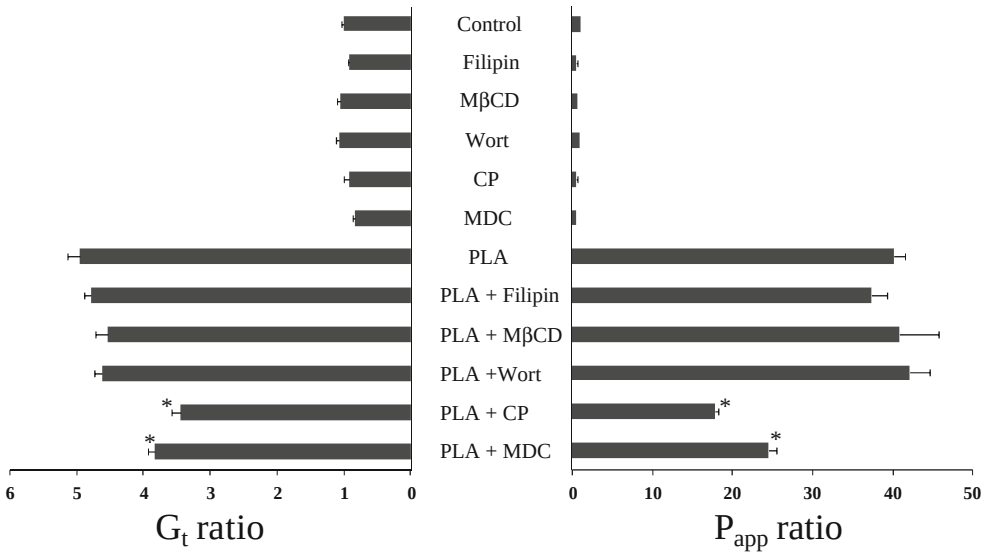

Fig. 1 The effects of PLA on the membrane conductance (G_t) and FD-4 permeation in the presence of endocytosis inhibitors in Caco-2 cell monolayers. G_t was calculated from TEER value 120 min after treatment with 100 μg/mL PLA in the presence of endocytosis inhibitors, and the ratio of the G_t in the treatment group to that in the control group (G_t ratio) was calculated. P_{app} was calculated from steady state flux of FD-4 after treatment with PLA in the presence of endocytosis inhibitors and the ratio of the P_{app} in the treatment group to that in the control group (P_{app} ratio) was calculated. Caveolae-mediated endocytosis inhibitors: filipin and MβCD. Macropinocytosis inhibitor: Wort. Clathrin-mediated endocytosis inhibitors: CP and MDC. Each data point represents the mean ± S.E. ($n = 4$). *$p < 0.05$ *vs.* PLA.

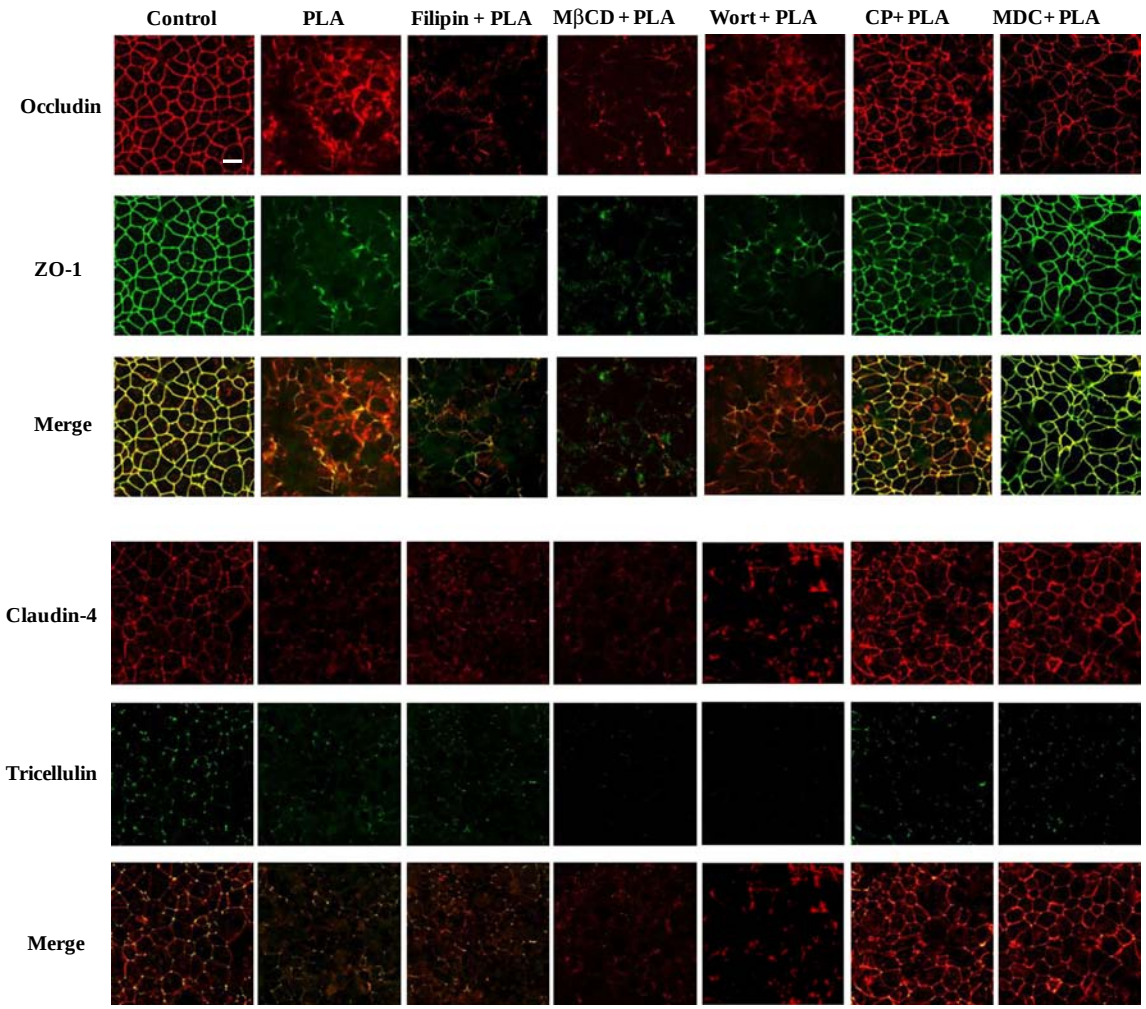

Fig. 2 The distribution of TJ proteins after treatment with 100 μg/mL PLA in the presence of endocytosis inhibitors. Immunofluorescence microscopic photographs of occludin, ZO-1, claudin-4 and tricellulin in Caco-2 cell monolayers. Caco-2 cells 120 min after treatment with 100 μg/mL PLA in the presence of endocytosis inhibitors were co-stained with anti occludin antibody, and anti ZO-1 antibody (*green*), anti claudin-4 antibody (*red*) or anti tricellulin antibody (*green*). Caveolae-mediated endocytosis inhibitors: filipin and MβCD. Macropinocytosis inhibitor: Wort. Clathrin-mediated endocytosis inhibitors: CP and MDC. Scale bar indicates 10 μm.

Figure 4 shows the G_t ratio and P_{app} ratio of erythritol after co-treatment of the Caco-2 monolayers with CP and PLA. These values were significantly reduced compared with that following treatment with PLA alone (85% and 83%, respectively).

Subcellular Distribution of Occludin After PLA Treatment

Figure 5 shows the distribution of occludin and clathrin after the treatment of Caco-2 cell monolayers with 100 μg/mL PLA. Occludin was located in cell–cell junctions, but clathrin did not co-localize in the cell–cell junctions under the control condition (0 min) (Fig. 5, left panels). In contrast, occludin partially disappeared from cell–cell junctions and clathrin was localized in the intercellular spaces 30 min after PLA treatment (Fig. 5, middle panels). A closer analysis demonstrated that occludin colocalized with clathrin in the intercellular spaces, as indicated by white arrows in the figure. Both occludin and clathrin disappeared from the intercellular space 60 min after PLA treatment (Fig. 5, right panels).

Figure 6 shows the distribution of occludin and endosomal proteins (early endosome marker: EEA-1, late endosome marker: LAMP-1, and recycling endosome marker: Rab11) 30 and 60 min after exposure of Caco-2 monolayers to 100 μg/mL PLA. Occludin was not colocalized with endosomal proteins before PLA treatment (Fig. 6, left panels). However, after the application of PLA, occludin colocalized with EEA1 and Rab11 in the intracellular space (Fig. 6, middle and right panels, white arrows). However, LAMP-1 did not colocalize with occludin at any of the tie points examined.

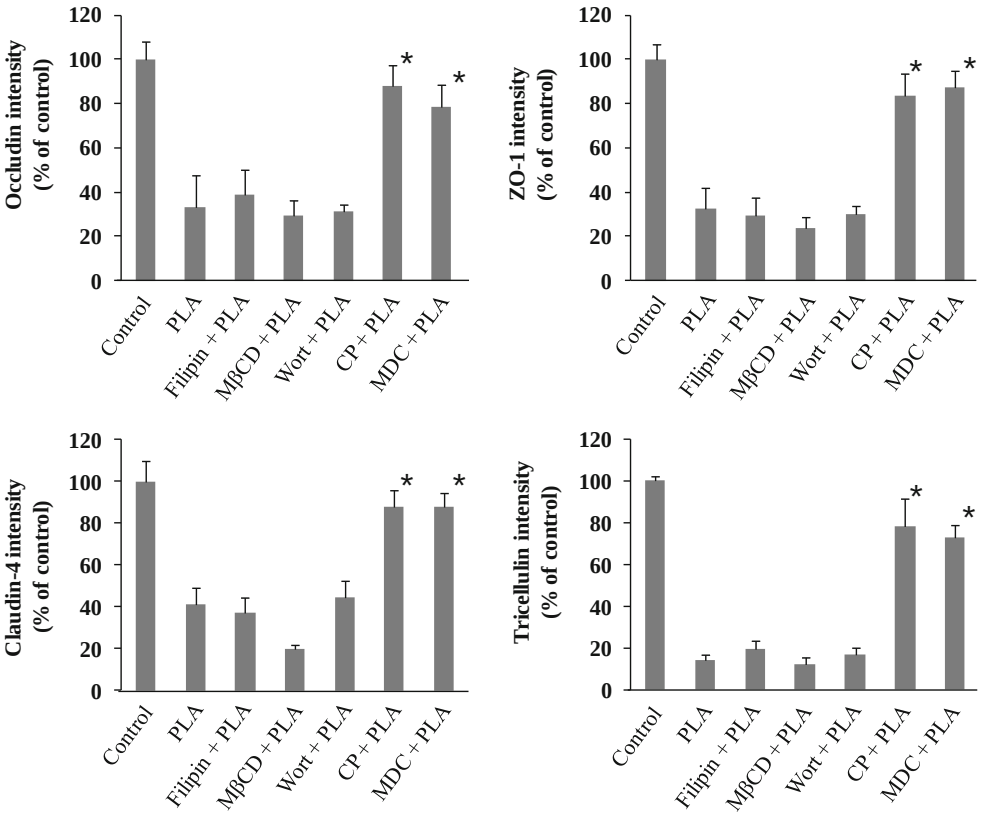

Fig. 3 The changes in the TJ protein levels after treatment of Caco-2 monolayers with PLA in the presence of endocytosis inhibitors. Immunofluorescence microscopic photographs of TJ proteins in Caco-2 cell monolayers. The junctional fluorescence intensity of TJ proteins 120 min after treatment with 100 μg/mL PLA in the presence of endocytosis inhibitors was determined by the Image J software program. Caveolae-mediated endocytosis inhibitors: filipin and MβCD. Macropinocytosis inhibitor: Wort. Clathrin-mediated endocytosis inhibitors: CP and MDC. Each data point represents the mean ± S.E. ($n = 4$). *$p < 0.05$ *vs.* PLA.

DISCUSSION

In the present study, we investigated that the mechanism underlying the disappearance of TJ proteins from cell–cell junctions using endocytosis inhibitors, and also examined the subcellular distribution of occludin, one of the TJ proteins. We demonstrated that the increased G_t and P_{app} of FD-4 after treatment of Caco-2 monolayers with PLA were significantly inhibited by clathrin-mediated endocytosis inhibitors (CP and MDC). In contrast, the effect of PLA on the G_t and P_{app} of FD-4 were not affected by the inhibitors of caveolae-mediated endocytosis and macropinocytosis. In addition, the disappearance of TJ proteins (occludin, ZO-1, claudin-4, and tricellulin) from cell–cell junctions after treatment with PLA was also inhibited exclusively by clathrin-mediated endocytosis inhibitors. Moreover, occludin was colocalized with clathrin in the intercellular spaces 30 min after the treatment of cells with PLA. Hence, the internalization of TJ proteins via clathrin-mediated endocytosis induced by PLA increased the paracellular permeability of Caco-2 cell monolayers to FD-4. These results suggest that clathrin-mediated endocytosis plays an important role in the internalization of TJ proteins induced by PLA.

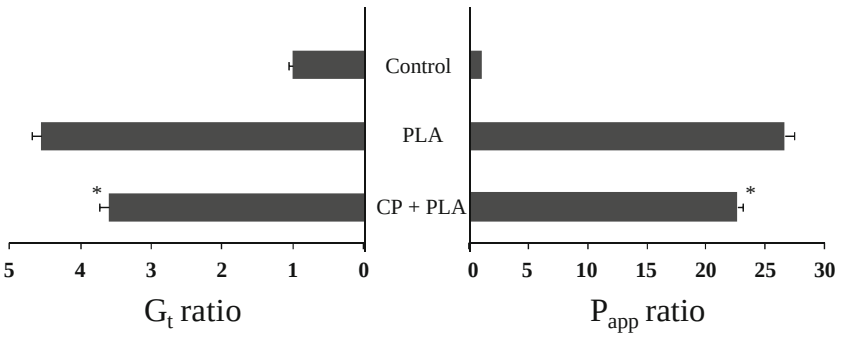

Fig. 4 The effects of PLA on the erythritol permeation in the presence of clathrin-mediated endocytosis inhibitors in Caco-2 cell monolayers. G_t was calculated from TEER value 120 min after treatment with 100 μg/mL PLA in the presence of CP, and the ratio of the G_t in the treatment group to that in the control group (G_t ratio) was calculated. P_{app} was calculated from steady state flux of erythritol after treatment with PLA in the presence of CP, and the ratio of the P_{app} in the treatment group to that in the control group (P_{app} ratio) was calculated. Each data point represents the mean ± S.E. ($n = 4$) *$p < 0.05$ *vs.* Control. $^{\dagger}p < 0.05$ *vs.* PLA.

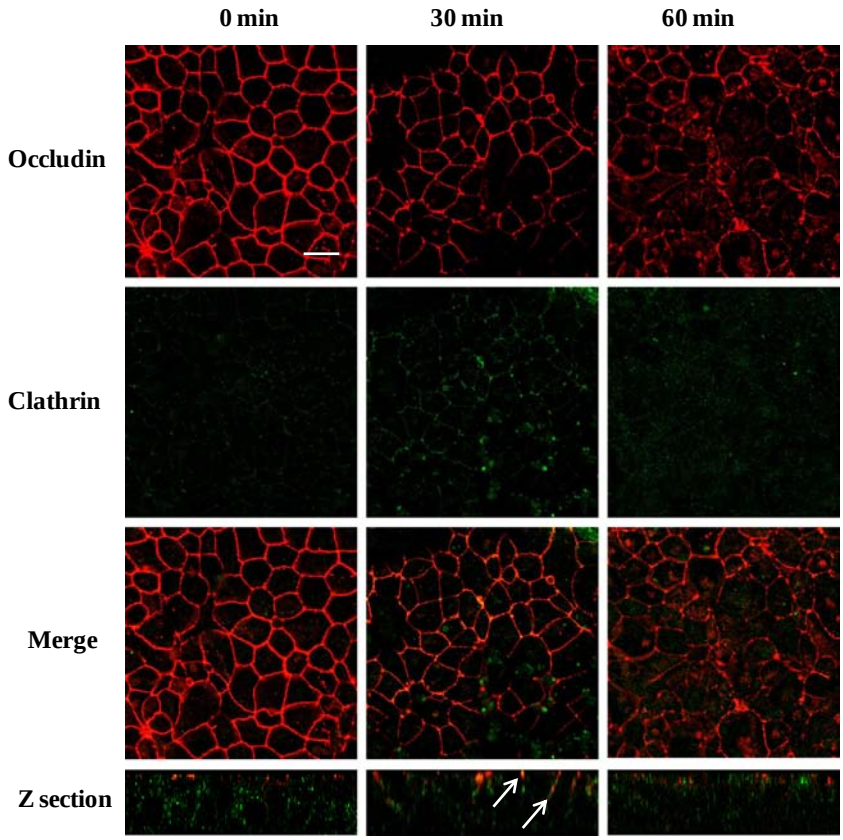

Fig. 5 The time-dependent changes in the distribution of clathrin and occludin after treatment of Caco-2 monolayers with PLA. Immunofluorecence microscopic photographs of clathrin and occludin in Caco-2 cell monolayers. Caco-2 cells were co-stained with anti clathrin (*green*) or occludin (*red*) after treatment with 100 μg/mL PLA. Scale bar indicates 10 μm.

Although the disappearance of TJ proteins from cell–cell junctions by PLA was suppressed by inhibiting clathrin-mediated endocytosis, the increase in the P_{app} of FD-4 was inhibited by only about half. Moreover, the increase in the G_t by PLA was only slightly inhibited by CP and MDC, although the G_t significantly decreased. In the previous work, a good linear relationship between the G_t and P_{app} of FD-4 was observed, when the effect of PLA concentration was

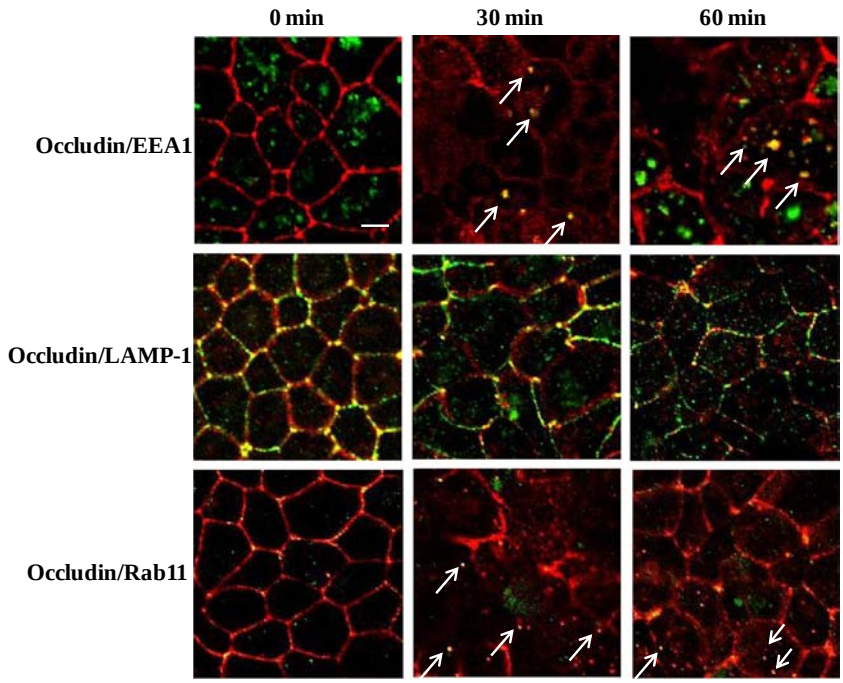

Fig. 6 The colocalization of occludin with endosome marker proteins after treatment of Caco-2 cell monolayers with PLA. Immunofluorecence microscopic photographs of occludin, EEA1, LAMP-1 and Rab11 in Caco-2 cell monolayers. Colocalization was assessed by immunostaining occludin (*red*) and endosome marker proteins (*green*) in Caco-2 cells 60 min after treatment with PLA. Scale bar indicates 10 μm.

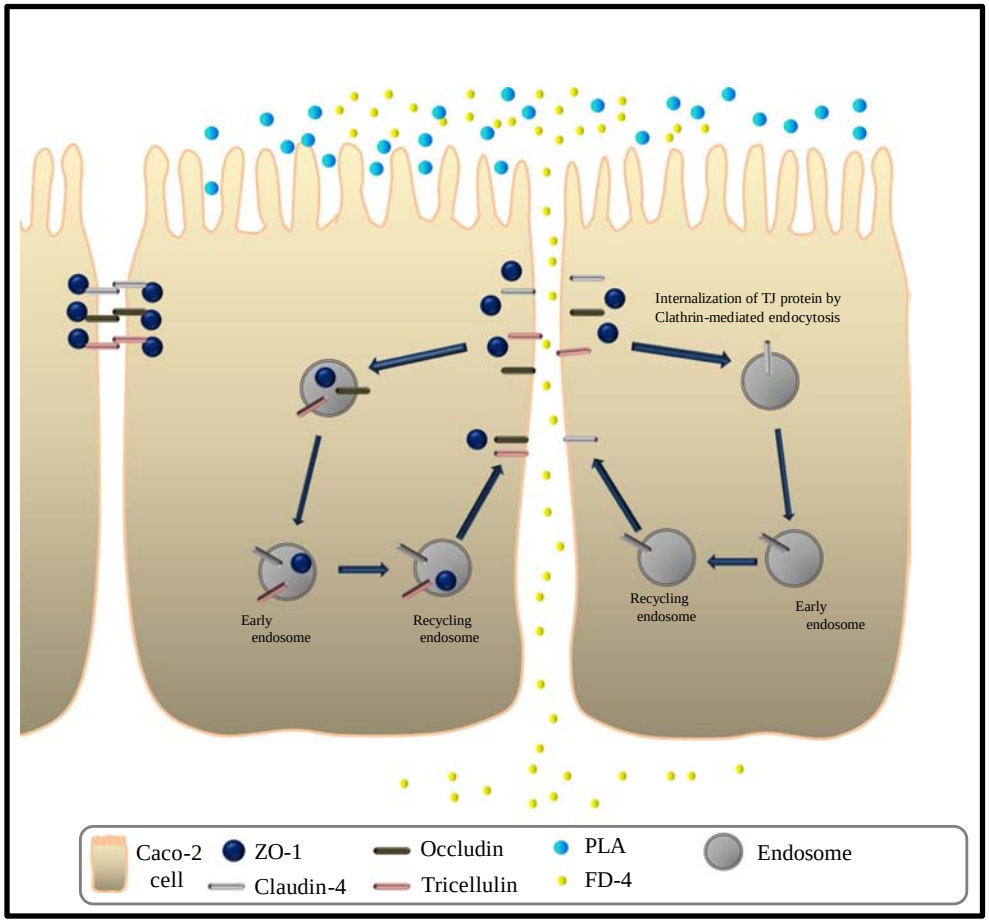

Fig. 7 A hypothetical schematic diagram of the internalization and recycling mechanisms of TJ proteins induced by PLA in Caco-2 cell monolayers.

investigated (14). However, the G_t ratio and P_{app} ratio of FD-4 following application of the clathrin-mediated endocytosis inhibitors were not matched in the present study. These results were inconsistent with those in the previous study. We speculated that the TJ strand structures were changed due to the loss of or changes in the interactions between TJ proteins induced by PLA, even though the endocytosis of these proteins was inhibited by the inhibitors. It was thus assumed that ions and low molecular compounds would be able to penetrate better than macromolecules through the paracellular space in the presence of clathrin-mediated endocytosis inhibitors. Therefore, a low molecular substance, erythritol, was used to demonstrate our hypothesis in a permeation study.

As a result of these studies, the increase in the P_{app} of erythritol induced by PLA in the presence of a clathrin-mediated endocytosis inhibitor, CP, was significantly reduced compared with that induced by treatment with PLA alone. The ratio of the P_{app} and G_t to those of the cells treated with PLA alone were 85% and 83%, respectively, which were closely similar values.

These results indicate that ions and low molecular substances could sufficiently penetrate through the paracellular space opened by PLA even in the presence of clathrin-mediated endocytosis inhibitors, suggesting that the effect of PLA on the G_t could be slightly (but not completely) inhibited by clathrin-mediated endocytosis inhibitors. In addition, the structural alterations in the TJ strand, in which TJ proteins still remained in cell–cell junctions after treatment with PLA in combination with clathrin-mediated endocytosis inhibitors, were found to form small pores where the small molecules, but not macromolecules, could enter. Moreover, it is possible that other claudins also disappeared from cell-cell junctions after treatment with PLA. Therefore, further investigation will be needed.

Our previous studies demonstrated that the expression of occludin was reduced by approximately 25% after PLA treatment in Caco-2 cell monolayers, indicating that occludin was partially degraded (14). In addition, the degradation of occludin was previously reported to occur when retinal endothelial cells and Caco-2 cell monolayers were treated with vascular endothelial growth factor (VEGF), tumor necrosis factor-α (TNF-α), and interleukin-1β (IL-1β) (15,26). Moreover, occludin plays a crucial role in the regulation of hydrophilic macromolecule penetration (12,27). Therefore, we investigated the subcellular distribution of occludin after treatment of Caco-2 cell monolayers with PLA. Our findings showed that occludin colocalized with an early endosome protein, EEA1, and a recycling endosome protein, rab11.

These results suggest that the occludin internalized by PLA treatment was transported to the early endosome, and then carried to the recycling endosome, where it finally might be recycled to cell–cell junctions. Additionally, other TJ proteins (ZO-1, claudin-4, and tricellulin) might also be recycled by the same route, because these TJ proteins were not degraded following their internalization following PLA treatment (14).

The present findings may be of interest in the fields of medical science and physiology, and may be useful for the further development of novel drug delivery strategies.

CONCLUSION

In the present study, we provided the first evidence of the internalization by clathrin-mediated endocytosis and recycling of TJ proteins in cell–cell junctions after treatment of Caco-2 cells with PLA. Figure 7 shows a possible mechanism of internalization of TJ proteins and the mechanism by which they are recycled after treatment with PLA. PLA induced an internalization of TJ proteins via clathrin-mediated endocytosis. As a result, the paracellular permeability of hydrophilic macromolecules was enhanced. The internalized TJ proteins were translocated to the early endosome and were subsequently transported to the recycling endosome. Hence, the reassembly of the TJ may involve the endosome pathway.

REFERENCES

1. Westergren I, Johansson BB. Altering the blood–brain barrier in the rat by intracarotid infusion of polycations: a comparison between protamine, poly-L-lysine and poly-L-arginine. Acta Physiol Scand. 1993;149(1):99–104.
2. Kotze AF, Luessen HL, de Leeuw BJ, deBoer AG, Verhoef JC, Junginger HE. Comparison of the effect of different chitosan salts and N-trimethyl chitosan chloride on the permeability of intestinal epithelial cells (Caco-2). J Control Release. 1998;51(1):35–46.
3. Sandri G, Poggi P, Bonferoni MC, Rossi S, Ferrari F, Caramella C. Histological evaluzation of buccal penetration enhancement properties of chitosan and trimethyl chitosan. J Pharm Pharmacol. 2006;58(10):1327–36.
4. McEwan G, Jepson M, Hirst BH, Simmons NL. Polycation-induced enhancement of epithelial paracellular permeability is independent of tight junctional characteristics. Biochim Biophys Acta. 1993;1148(1):51–60.
5. Artursson P, Lindmark T, Davis SS, Illum L. Effect of chitosan on the permeability of monolayers of intestinal epithelial cells (Caco-2). Pharm Res. 1994;11(9):1358–61.
6. Natsume H, Iwata S, Ohtake K, Miyamoto M, Yamaguchi M, Hosoya K, *et al.* Screening of cationic compounds as an absorption enhancer for nasal drug delivery. Int J Pharm. 1999;185(1):1–12.
7. Ohtake K, Maeno T, Ueda H, Ogihara M, Natsume H, Morimoto Y. Poly-L-arginine enhances paracellular permeability via serine/threonine phosphorylation of ZO-1 and tyrosine dephosphorylation of occludin in rabbit nasal epithelium. Pharm Res. 2003;20(11):1838–45.
8. Furuse M, Itoh M, Hirase T, Nagafuchi A, Yonemura S, Tsukita S, *et al.* Direct association of occludin with ZO-1 and its possible involvement in the localization of occludin at tight junctions. J Cell Biol. 1994;127(6 Pt 1):1617–26.
9. Furuse M, Fujita K, Hiiragi T, Fujimoto K, Tsukita S. Claudin-1 and -2: novel integral membrane proteins localizing at tight junctions with no sequence similarity to occludin. J Cell Biol. 1998;141(7):1539–50.
10. Furuse M, Sasaki H, Fujimono K, Tsukita S. A single gene product, claudin-1 or -2, reconstitutes tight junction strands and recruits occludin in fibroblasts. J Cell Biol. 1998;143(2):391–401.
11. Simon DB, Lu Y, Choate KA, Velazquez H, AL-Sabban E, Praga M, *et al.* Paracellin-1 a renal tight junction protein required for paracellular Mg^{2+} resorption. Science. 1999;285(5424):103–6.
12. Al-Sadi R, Khatib K, Guo S, Youssef M, Ma T. Occludin regulates macromolecule flux across the intestinal epithelial tight junction barrier. Am J Physiol Gastrointest Liver Physiol. 2011;300(6):G1054–64.
13. Ikenouchi J, Furuse M, Furuse K, Sasaki H, Tsukita S, Tsukita S. Tricellulin constitutes a novel barrier at tricellular contacts of epithelial cells. J Cell Biol. 2005;171(6):939–45.
14. Yamaki T, Ohtake K, Ichikawa K, Uchida M, Uchida H, Ohshima S, *et al.* Poly-L-arginine-induced internalization of tight junction proteins increases the paracellular permeability of the Caco-2 cell monolayer to hydrophilic macromolecules. Biol Pharm Bull. 2013;36(3):432–41.
15. Murakami T, Felinski EA, Antonetti DA. Occludin phosphorylation and ubiquitination regulate tight junction trafficking and vascular endothelial growth factor-induced permeability. J Biol Chem. 2009;284(31):21036–46.
16. Ivanov AL, Nusrat A, Parkos CA. Endocytosis of epithelial apical junctional proteins by a clathrin-mediated pathway into a unique storage compartment. Mol Biol Cell. 2004;15(1):176–88.
17. Stamatovic SM, Keep RF, Wang MM, Jankovic I, Andjelkovic AV. Caveolae-mediated internalization of occludin and claudin-5 during CCL2-induced tight junction remodeling in brain endothelial cells. J Biol Chem. 2009;284(28):19053–66.
18. Bruewer M, Utech M, Ivanov AL, Hopkins AM, Parkos CA, Nusrat A. Interferon-gamma induces internalization of epithelial tight junction proteins via a macropinocytosis-like process. FASEB. 2005;19(8):923–33.
19. Conner SD, Schmid SL. Regulated portals of entry into the cell. Nature. 2003;422(6927):37–44.
20. Utech M, Mennigen R, Bruewer M. Endocytosis and recycling of tight junction proteins in inflammation. J Biomed Biotechnol. 2010;2010:484987.
21. Liu J, Kesiry R, Periyasamy SM, Malhotra D, Xie Z, Shapiro JI. Ouabain induces endocytosis of plasmalemmal Na/K-ATPase in LLC-PK1 cells by a clathrin-dependent mechanism. Kidney Int. 2004;66(1):227–41.
22. Kim Y, Kugler MC, Wei Y, Kim KK, Li X, Brumwell AN, *et al.* Integrin alpha3beta1-dependent beta-catenin phosphorylation links epithelial Smad signaling to cell contacts. J Cell Biol. 2009;184(2):309–22.
23. Seki T, Kiuchi T, Seto H, Kimura S, Egawa Y, Ueda H, *et al.* Analysis of the rat skin permeation of hydrophilic compounds using the Renkin function. Biol Pharm Bull. 2010;33(11):1915–8.
24. Seth A, Sheth P, Elias BC, Rao R. Protein phosphatases 2A and 1 interact with occludin and negatively regulate the assembly of tight junctions in the CACO-2 cell monolayer. J Biol Chem. 2007;282(15):11487–98.
25. Mohammad-Panah R, Ackerley C, Rommens J, Choudhury M, Wang Y, Bear CE. The chloride channel CIC-4 co-localizes with cystic fibrosis transmembrane conductance regulator and may mediate chloride flux across the apical membrane of intestinal epithelia. J Biol Chem. 2002;277(1):566–74.

26. Al-Sadi RM, Ma TY. IL-1beta causes an increase in intestinal epithelial tight junction permeability. J Immunol. 2007;178(7): 4641–9.

27. Ye D, Guo S, Al-Sadi R, Ma TY. MicroRNA regulation of intestinal epithelial tight junction permeability. Gastroenterology. 2011;141(4): 1323–33.